AD-A159 058 TRANSVERSE MOTION OF HIGH SPEED BARIUM CLOUDS IN THE IONOSPHERE(U) NAVAL RESEARCH LAB WASHINGTON DC H G MITCHELL ET AL. 18 SEP 85 NRL-MR-5626 1/1

UNCLASSIFIED F/G 4/1 NL

END

FILMED

DTIC

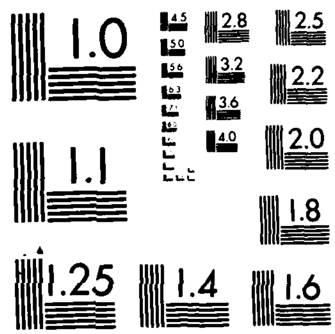

MICROCOPY RESOLUTION TEST CHART

NATIONAL BUREAU OF STANDARDS 1963 A

NRL Memorandum Report 5626

AD-A159 058

Transverse Motion of High Speed Barium Clouds in the Ionosphere

H. G. MITCHELL,* J. A. FEDDER, J. D. HUBA AND S. T. ZALESAK

Geophysical and Plasma Dynamics Branch
Plasma Physics Division

**Science Applications International Corporation*
McLean, VA 22102

September 18, 1985

This research was supported by the National Aeronautics and Space Administration.

NAVAL RESEARCH LABORATORY
Washington, D.C.

AD-A159058

SECURITY CLASSIFICATION OF THIS PAGE

REPORT DOCUMENTATION PAGE

1a. REPORT SECURITY CLASSIFICATION UNCLASSIFIED	1b. RESTRICTIVE MARKINGS
2a. SECURITY CLASSIFICATION AUTHORITY	3. DISTRIBUTION/AVAILABILITY OF REPORT Approved for public release; distribution unlimited.
2b. DECLASSIFICATION / DOWNGRADING SCHEDULE	
4. PERFORMING ORGANIZATION REPORT NUMBER(S) NRL Memorandum Report 5626	5. MONITORING ORGANIZATION REPORT NUMBER(S)
6a. NAME OF PERFORMING ORGANIZATION Naval Research Laboratory — 6b. OFFICE SYMBOL (If applicable) Code 4780	7a. NAME OF MONITORING ORGANIZATION
6c. ADDRESS (City, State, and ZIP Code) Washington, DC 20375-5000	7b. ADDRESS (City, State, and ZIP Code)
8a. NAME OF FUNDING/SPONSORING ORGANIZATION NASA — 8b. OFFICE SYMBOL (If applicable) EEA	9. PROCUREMENT INSTRUMENT IDENTIFICATION NUMBER
8c. ADDRESS (City, State, and ZIP Code) Washington, DC 20546	10. SOURCE OF FUNDING NUMBERS PROGRAM ELEMENT NO. H-83200-B; PROJECT NO.; TASK NO.; WORK UNIT ACCESSION NO. DN155-233

11. TITLE (Include Security Classification)
Transverse Motion of High Speed Barium Clouds in the Ionosphere

12. PERSONAL AUTHOR(S)
Mitchell, H.G.,* Fedder, J.A., Huba, J.D. and Zalesak, S.T.

13a. TYPE OF REPORT	13b. TIME COVERED	14. DATE OF REPORT (Year, Month, Day)	15. PAGE COUNT
Interim	FROM ______ TO ______	1985 September 18	20

16. SUPPLEMENTARY NOTATION *Science Applications International Corporation, McLean, VA 22102
This research was supported by the National Aeronautics and Space Administration.

17. COSATI CODES			18. SUBJECT TERMS (Continue on reverse if necessary and identify by block number)
FIELD	GROUP	SUB-GROUP	Barium cloud; Plasma injection; Ionospheric modeling

19. ABSTRACT (Continue on reverse if necessary and identify by block number)

Simulation results, based on a field-line-integrated, 2D, electrostatic model, are presented for the motion of a barium cloud injected transverse to the geomagnetic field in the ionosphere at high speeds. It is found that the gross evolution of injected plasma clouds depends sensitively on the initial conditions, as well as the nature of the background coupling. For a massive ($M_O \sim 10$ kg), orbital ($V_O \sim 5$ km/sec) release in the F region (350-450 km), we find that plasma clouds can drift tens of kilometers across the magnetic field in tens of seconds after ionization.

20. DISTRIBUTION/AVAILABILITY OF ABSTRACT ☒ UNCLASSIFIED/UNLIMITED ☐ SAME AS RPT ☐ DTIC USERS	21. ABSTRACT SECURITY CLASSIFICATION UNCLASSIFIED
22a. NAME OF RESPONSIBLE INDIVIDUAL J. D. Huba	22b. TELEPHONE (Include Area Code) (202) 767-3630 — 22c. OFFICE SYMBOL Code 4780

DD FORM 1473, 84 MAR — 83 APR edition may be used until exhausted. All other editions are obsolete.

SECURITY CLASSIFICATION OF THIS PAGE

CONTENTS

TRANSVERSE MOTION OF HIGH SPEED BARIUM CLOUDS IN THE IONOSPHERE

I. INTRODUCTION

The evolution of artificial plasma clouds in the earth's ionosphere has been under scientific investigation for more than two decades. A variety of experimental, theoretical, and computational research programs have been carried out, and research in this area remains active. One interesting problem that requires further investigation is the dynamics of a high speed plasma cloud moving transverse to the ambient geomagnetic field. Experimentally this phenomenon has been studied using shaped charge barium releases (Wescott et al., 1980; Simons et al., 1980; Koons and Pongratz, 1981) and rocket barium releases (Mende, 1973; Brence et al., 1973; Heppner et al., 1981), and will be a major part of the scientific studies for the upcoming CRRES mission (Combined Release and Radiation Effects Satellite) sponsored by NASA and the Air Force. It should be noted that the high speed releases to date have been relatively small (barium vapor less than 1 kg) compared to those planned for the CRRES mission (up to 10 kg of barium vapor). Theoretically this problem has been addressed by Scholer (1970) for magnetospheric releases, and Sperling (1983) for ionospheric releases using simple, idealized cloud models. However, to our knowledge, no studies or simulations have been performed to study this phenomenon for more realistic 2D cloud models.

In this paper, we present results of numerical simulations based on a 2D, electrostatic model which describe the gross motion of a massive barium release injected transverse to the geomagnetic field at a high velocity. Since our model is electrostatic, we limit our attention to small kinetic beta clouds, i.e., $\beta_k << 1$ where $\beta_k = 1/2\ n_i m_i V^2/(B^2/8\pi)$, and neglect any MHD perturbations generated by the injected cloud. Our primary interest is to determine whether or not injected plasma clouds can "skid" across the magnetic field, and if so, what physical processes control this behavior. We find that the gross motion of injected clouds depend sensitively on initial conditions, as well as the nature of the background coupling. For the case of a massive barium release ($M_0 \sim 10$ kg) in the F-region (350-450 km) at orbital velocity ($V_0 \lesssim 5$ km/sec), we predict that the plasma cloud

Manuscript approved June 4, 1985.

can drift tens of kilometers on a time scale of tens of seconds after ionization.

II. MODEL AND EQUATIONS

We use a slab geometry such that the ambient geomagnetic field is in the z-direction $(\underset{\sim}{B} = B_0 \, e_z)$ and a neutral barium cloud is injected transverse to $\underset{\sim}{B}$ in the y-direction $(\underset{\sim}{V}_n = V_0 \, e_y)$. The barium subsequently becomes ionized by either photoionization or Alfvén's critical velocity ionization mechanism; we only consider the former in this letter. We now describe the neutral and plasma cloud models in more detail.

Neutral Cloud Evolution:

The model we use to describe the evolution of the neutral cloud transverse to $\underset{\sim}{B}$ is relatively simple. The basic processes we consider are self-diffusion of the neutral barium cloud, slowing down of the cloud because of collisions with the background ionosphere, and a neutral loss due to photoionization. Assuming that the neutral cloud initially has a Gaussian density profile, the time evolution of the field-line-integrated density is approximately described by

$$n_n(\underset{\sim}{r}, t) = \frac{M_0}{m\pi r_D^2(t)} \exp \left\{- \frac{(\underset{\sim}{r} - \underset{\sim}{x}(t))^2}{r_D^2(t)} - \sigma_i t\right\} \tag{1}$$

where

$$\underset{\sim}{v}(t) = \underset{\sim}{V}_n \exp(- \nu_s t) \tag{2}$$

$$\underset{\sim}{x}(t) = \underset{\sim}{x}_0 + [1 - \exp(- \nu_s t)]\underset{\sim}{V}_n/\nu_s \tag{3}$$

$$r_D(t) = (r_0^2 + 4Dt)^{1/2}, \tag{4}$$

$\underset{\sim}{r}$, $\underset{\sim}{x}$, and $\underset{\sim}{v}$ refer only to the perpendicular components, the subscript n denotes neutrals, M_0 is the initial total mass, σ_i is the ionization loss rate, ν_s is the collision frequency associated with the slowing down of the cloud, $\underset{\sim}{V}_n = V_0 \, e_y$ is the injection velocity at $t = 0$, r_0 is the cloud radius at $t = 0$, $\underset{\sim}{x}_0$ is the cloud center position at $t = 0$, and D is the diffusion coefficient ($D = T/m\nu_D$, where T is temperature, m is the mass, and ν_D is the collision frequency for diffusion). In deriving (1)-(4) we have made the assumption that the slowing down process and the self-diffusion process are independent of each other. Although this assumption is certainly an over-simplification of the neutral dynamics, we have made it because we are primarily interested in the ion cloud dynamics and it leads to a relatively simple description of the neutral cloud.

Plasma Cloud Evolution:

We assume that the plasma cloud is generated by photoionization of the neutral cloud. This ionization contributes a source term of the form $\sigma_i n_n$ to the ion continuity equation and one of the form $m_i \sigma_i n_n (\underset{\sim}{v} - \underset{\sim}{v}_i)$ to the ion momentum equation, where σ_i is the ionization production rate. Upon ionization, the ions and electrons have a large initial velocity and gyrate about the ambient magnetic field in opposite directions, leading to a source Pedersen current density $\underset{\sim}{j}_s$. This causes excess charge to pile-up on the edges of the cloud, and produces a polarization electric field across the cloud. This field leads to an $\underset{\sim}{E} \times \underset{\sim}{B}$ drift of the plasma cloud in the direction of the neutral cloud motion.

In order to describe this behavior quantitatively we use a field-line-integrated, two-layer, electrostatic model. We consider a cloud layer and a background ionosphere layer which are coupled by the ambient magnetic field lines, assumed to be equipotentials. Note that we neglect any MHD perturbations that may have been generated by the ion cloud. The equations which describe this model are the following:

$$\frac{\partial n_c}{\partial t} + \nabla \cdot \left(n_c \underset{\sim}{v}_i\right) = \sigma_i \, n_n \tag{5}$$

$$\underset{\sim}{v}_i = \underset{\sim}{v}_e = - \frac{c\nabla\phi}{B} \times e_z \tag{6}$$

$$\underset{\sim}{j}_s = - \sigma_{ps} \nabla\phi + \frac{B}{c} \sigma_{ps} \underset{\sim}{v} \times e_z \tag{7}$$

$$\underset{\sim}{j}_c = - \sigma_{pc} \nabla\phi - \frac{1}{4\pi} \frac{c^2}{V_{Ac}^2} \left(\frac{\partial}{\partial t} + \underset{\sim}{v}_i \cdot \nabla\right) \nabla\phi \tag{8}$$

$$\underset{\sim}{j}_b = - \sigma_{pb} \nabla\phi - \frac{1}{4\pi} \frac{c^2}{V_{Ab}^2} \left(\frac{\partial}{\partial t} + \underset{\sim}{v}_i \cdot \nabla\right) \nabla\phi \tag{9}$$

where $\sigma_{pc(b)} = (ce/B)(n_i\nu_{in}/\Omega_i)_{c(b)}$ is the Pedersen conductivity of the cloud (background), $\sigma_{ps} = (ce/B)(n_n\sigma_i/\Omega_i)$ is the source function for Pedersen conductivity caused by ionization, ν_{in} is the ion-neutral collision frequency, $V_{Ac(b)} = B/(4\pi n m_i)^{1/2}$ is the Alfvén velocity in the cloud (background), Ω_i is the ion cyclotron frequency, and ∇ refers to only the perpendicular components. The perpendicular currents in the cloud $(\underset{\sim}{j}_c)$ and background $(\underset{\sim}{j}_b)$ are assumed to close via parallel electron currents.

Making use of (5)-(9), we assume that the source Pedersen currents close by Pedersen and polarization currents in the cloud and in the background, and so integrate $\nabla\cdot\underset{\sim}{j} = 0$ along the field lines to obtain the potential equation

$$\nabla \cdot \{\Sigma_{pc}[1 + \nu_{in}^{-1}(\frac{\partial}{\partial t} + \underset{\sim}{v}_i \cdot \nabla)]\nabla\phi$$

$$+ \Sigma_{pb}\nabla\phi + C_b(\frac{\partial}{\partial t} + \underset{\sim}{v}_i \cdot \nabla)\nabla\phi\} \tag{10}$$

$$= -\nabla \cdot \{\Sigma_{ps}(\nabla\phi - \frac{B}{c}\underset{\sim}{v} \times e_z)\}$$

where Σ_{pc}, Σ_{ps}, Σ_{pb} are the integrated Pedersen conductivities associated with the cloud, source, and background, respectively, and C_b is the integrated inertial capacitance associated with the background, i.e.,

$$C_b = \frac{1}{4\pi}\int_b dz\ (c^2/V_{Ab}^2).$$

We also rewrite (5) as a continuity equation for Σ_{pc}

$$\frac{\partial\ \Sigma_{pc}}{\partial t} + \nabla \cdot (\Sigma_{pc}\ \underset{\sim}{v}_i) = \nu_{in}\Sigma_{ps}. \tag{11}$$

The background layer is assumed incompressible so that its continuity equation can be neglected. Thus, the system is completely described by (1)-(4), (6), (10), and (11) in the variables Σ_{pc} and ϕ. It should be noted that these equations have not been used in large scale simulation codes to study plasma cloud motion in the ionosphere to date. The new feature in these equations is ion inertia, i.e., the terms associated with $(\partial/\partial t + \underset{\sim}{v} \cdot \nabla)$ in (10) and which lead to polarization curents.

Previous studies neglected these terms to study plasma cloud evolution because the time scales of interest were such that $\nu_{in} >> (\partial/\partial t + \underset{\sim}{v} \cdot \nabla)$ and inertial effects could be safely neglected [McDonald et al., 1981; Zalesak et al., 1985]. However, this approximation is not valid for the releases of interest (e.g., CRRES releases) and ion inertia must be considered.

III. SIMULATION RESULTS

The numerical methods used to simulate the model equations are described in Zalesak et al. (1982) and Mitchell et al. (1985). The continuity equation (11) is solved numerically using the multi-dimensional flux-corrected techniques of Zalesak (1979), while the potential equation (10) is solved with the incomplete Cholesky conjugate gradient algorithm of Hain (1980). The simulations are performed on a 80 x 100 cell grid (x,y) with a cell size of 1 km x 1 km.

We present the results of two simulations. The parameters used are the following: $B_0 = 0.4$ G, $\nu_D = \nu_s = \nu_{in} = \sigma_i = 0.04$ sec^{-1}, $r_0 = 2$ km, T = 0.1 eV, $M_0 = 10$ kg, $V_0 = 5$ km/sec, and $m_i = 137\ m_p$ (barium). These parameters are appropriate for a 350-450 km altitude release at mid-latitudes. The integrated Pedersen conductivity of the background is taken to be $\Sigma_{pb} = 1$ mho, and two values of the integrated inertial capacitance are chosen, $C_b = 0$ (case 1) and $C_b = 10$ farad (case 2).

Figure 1 shows the results for the case where $C_b = 0$. Physically this corresponds to source region currents closing via Pedersen currents. Figure 1a shows the integrated Pedersen conductance and velocity flow field for the ion cloud, and Figure 1b shows the corresponding electrostatic potential at times t = 1, 9, 19, and 25 sec after initialization. We also show the location of the neutral vapor by a solid circle of radius r_D. Note that the velocity vectors are normalized to the maximum velocity at each time step, and comparisons in the magnitude of the velocity at different times can only be made from the potentials. Two features are immediately apparent. First, at early times ($t \lesssim 3$ sec) the plasma and neutral clouds are nearly collocated, but the plasma decelerates more quickly than the neutral vapor. By 25 sec the high density portion of the plasma cloud has almost stopped drifting after traversing ~ 38 km across the field. Second, the region of strong electric fields remains in the source region, the neutral vapor cloud, and at later times only the low density leading edge of the plasma continues to drift rapidly. Moreover, the electric field strength in the source region monotonically decreases as the plasma production weakens and the cloud conductance increases.

Figure 2 shows the results for the case where C_b = 10 farad. Physically, this case has the source region currents close via Pedersen currents and polarization currents in the background plasma. Again, the Pedersen conductance and velocity field of the ion cloud, and the electrostatic potential are shown in Figures 2a and 2b, respectively, at the same times as in Figure 1. In comparing Figure 2 to Figure 1, three differences immediately stand out. First, the ion cloud in Figure 2 lags further behind the neutral vapor cloud than in Figure 1. Second, at later times, the potential for the second case decays more slowly in the dense portion of the ion cloud than it did in the first case. Third, the plasma cloud in the second case is bifurcated on its trailing edge. The differences between Figures 1 and 2 are the direct results of the inclusion of the background plasma inertia in case 2.

The evolution of the electric field and the ion cloud drift can be understood by consideration of (10). If we neglect inertial effects, as in case 1, the electric field in the production region is approximately $\underset{\sim}{E} = \Sigma_{ps}/(\Sigma_{pc} + \Sigma_{pb} + \Sigma_{ps})\ \underset{\sim}{V}_n \times \underset{\sim}{B}/c$. At early times the electric field in the source region is strong ($\sim 0.96\ \underset{\sim}{V}_n \times \underset{\sim}{B}/c$) but decreases rapidly as Σ_{ps} decreases and Σ_{pc} increases. The primary effect of the inertial terms is to cause the electric field in the dense portion of the cloud to decay with a time constant $\Sigma_{pc}/\nu_{in}(\Sigma_{pc} + \Sigma_{pb}) \sim 12$ sec. The ion cloud is decelerated relative to the neutral cloud because the background Pedersen currents (i.e., "line tying" currents) couple the ion cloud momentum to the higher density, low altitude neutral atmosphere. For the case 2, the inertial terms in (10) cannot be neglected. The source currents, in addition to closing via Pedersen conduction current, must now also close via polarization currents which set the background plasma into motion along with the ion cloud. The newly produced ions share their momentum with the background, and therefore the electric field in the source region is less than in case 1 (initially $E_2 \sim 0.6\ E_1$). Additionally, the background ionization inertia leads to a slower decay of plasma momentum outside the source region. The decay time constant for case 2 is $(C_b + \Sigma_{pc}/\nu_{in})/(\Sigma_{pc} + \Sigma_{pb}) \sim 16$ sec. Thus, at later times the electric field in the dense portion of the ion cloud for case 2 can be greater than that for case 1. The bifurcation of the trailing portion of the case 2 plasma cloud is the direct result of the spatial variation of the longer decay time constant. The denser portion of the ion cloud travels faster for a longer period of time than the less dense portion. This is clearly shown by comparing the regions of maximum velocity between case 1 and case 2.

IV. SUMMARY

We have presented a 2D, electrostatic model and simulation results for a plasma cloud injected transverse to the ambient geomagnetic field at high velocities (e.g., orbital velocity). Such a model is relevant to shaped charge and satellite barium releases, and to the proposed chemical release for the upcoming CRRES mission. From the results shown here and from other simulations of releases we have performed for different parameters, we find that the gross evolution of the plasma cloud depends on the initial conditions (i.e., M_0, V_0, etc.), as well as the nature of the background coupling. Plasma clouds that generate currents which close via Pedersen currents in the background ionosphere tend to drift further across the ambient field than those which have currents which also close via polarization currents. In either case though, it is predicted that the plasma clouds can drift tens of kilometers across the geomagnetic field after ionization for a massive barium release in the F region. In fact, recent analysis of the BUARO shaped charge release indicates that barium injected perpendicular to $\underline{B}$ at a velocity ~ 10 km/sec "skidded" ~ 50 km across the magnetic field (Pongratz, private communication, 1985) which is consistent with our simulations.

The problem studied here is similar in many respects to a previous investigation of the interaction of Io with its plasma torus by Goertz (1980). Goertz' paper was directed toward obtaining solutions for Alfvén wave generation and propagation for acceleration of ambient plasma on magnetic field lines which pass near Io, while using an approximation for the source region plasma and electric potential. Here, we are concerned with obtaining an accurate description for the source region plasma density and electric potential, while approximating the interaction with the ambient geomagnetic field line connected plasma. The two sets of results are complimentary and are consistent with each other.

The results shown and discussed above are not presented as a detailed, precise prediction of plasma cloud release behavior for a particular experiment. They do, however, demonstrate processes which are physically important for high velocity plasma cloud releases and must be considered in planning for future experiments such as those planned for the upcoming CRRES mission.

Acknowledgments

This research has been sponsored by NASA.

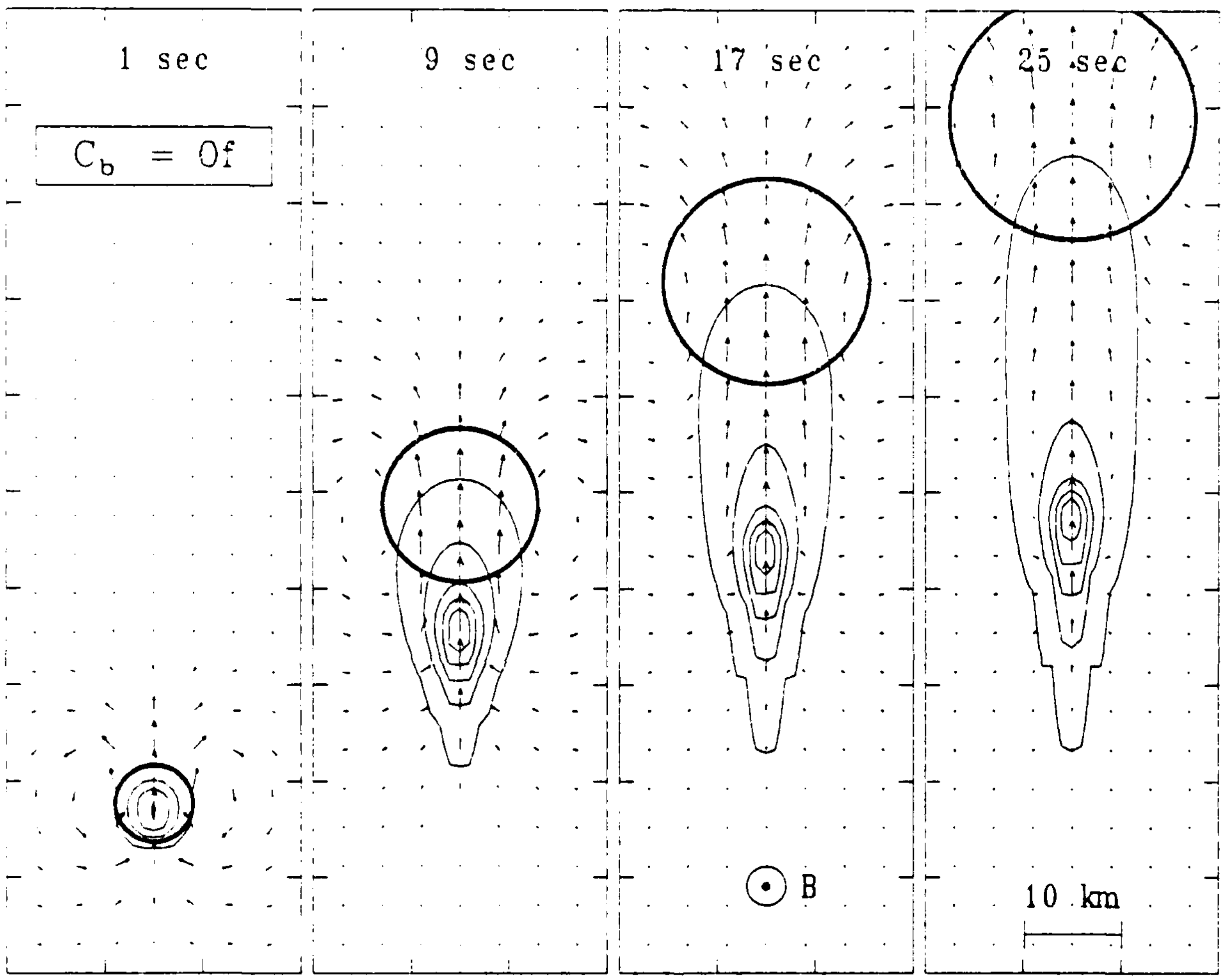

Fig. 1 — Contours of constant Σ_{pc}, velocity flow vectors, and electrostatic potential for the case $C_b = 0$ f. (a) Contours of constant Σ_{pc} and velocity flow vectors for t = 1, 9, 17, and 25 sec after initialization. The contour separation is .2 mho with the minimum contour at .1 mho, and the vectors are independently normalized for each time. The solid circle represents the location of the neutral vapor and has radius r_0. (b) Electrostatic potential contours for the times in (a). The potential difference between contours is 60 V.

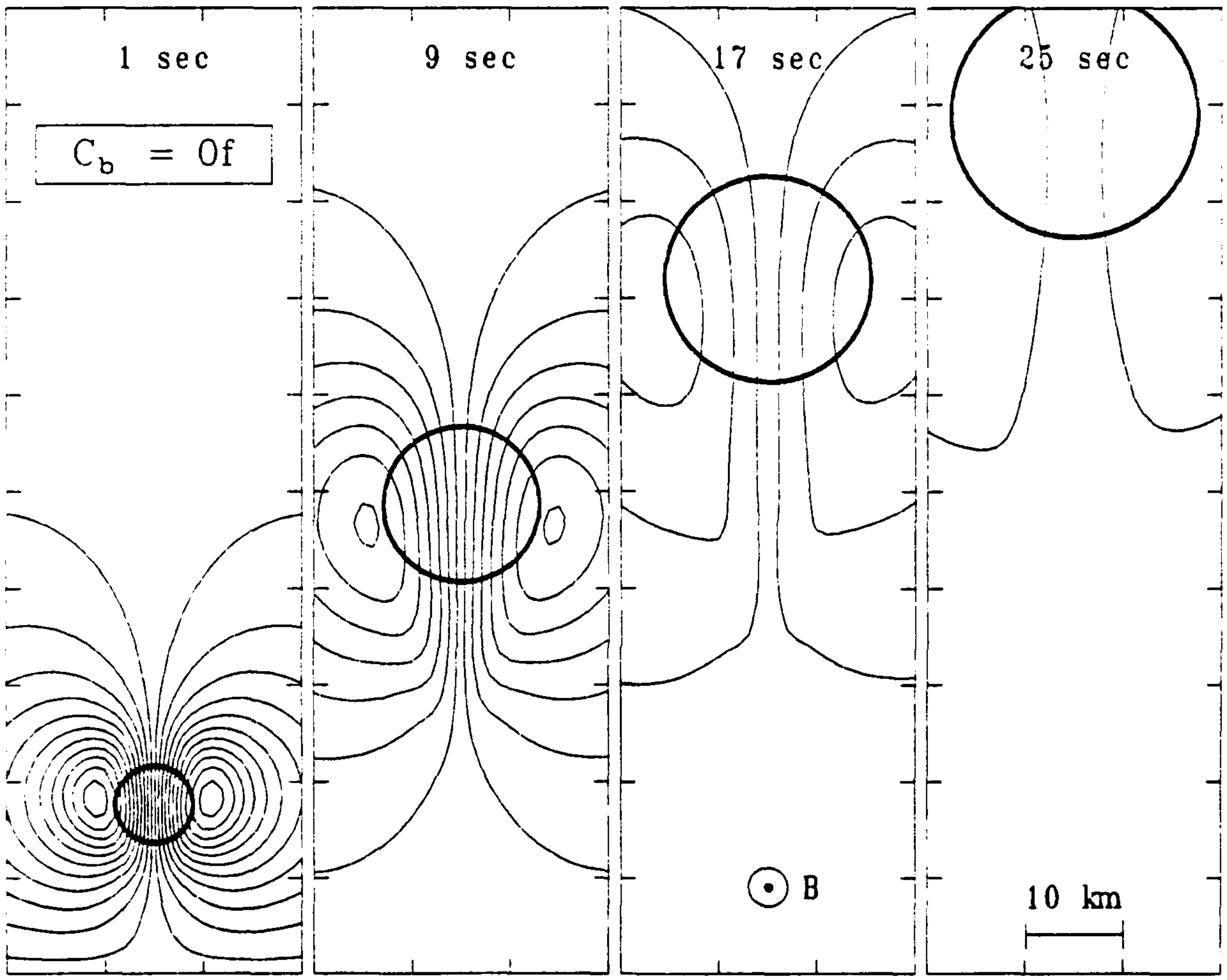

Fig. 1 (Cont'd) — Contours of constant Σ_{pc}, velocity flow vectors, and electrostatic potential for the case C_b = 0 f. (a) Contours of constant Σ_{pc} and velocity flow vectors for t = 1, 9, 17, and 25 sec after initialization. The contour separation is .2 mho with the minimum contour at .1 mho, and the vectors are independently normalized for each time. The solid circle represents the location of the neutral vapor and has radius r_D. (b) Electrostatic potential contours for the times in (a). The potential difference between contours is 60 V.

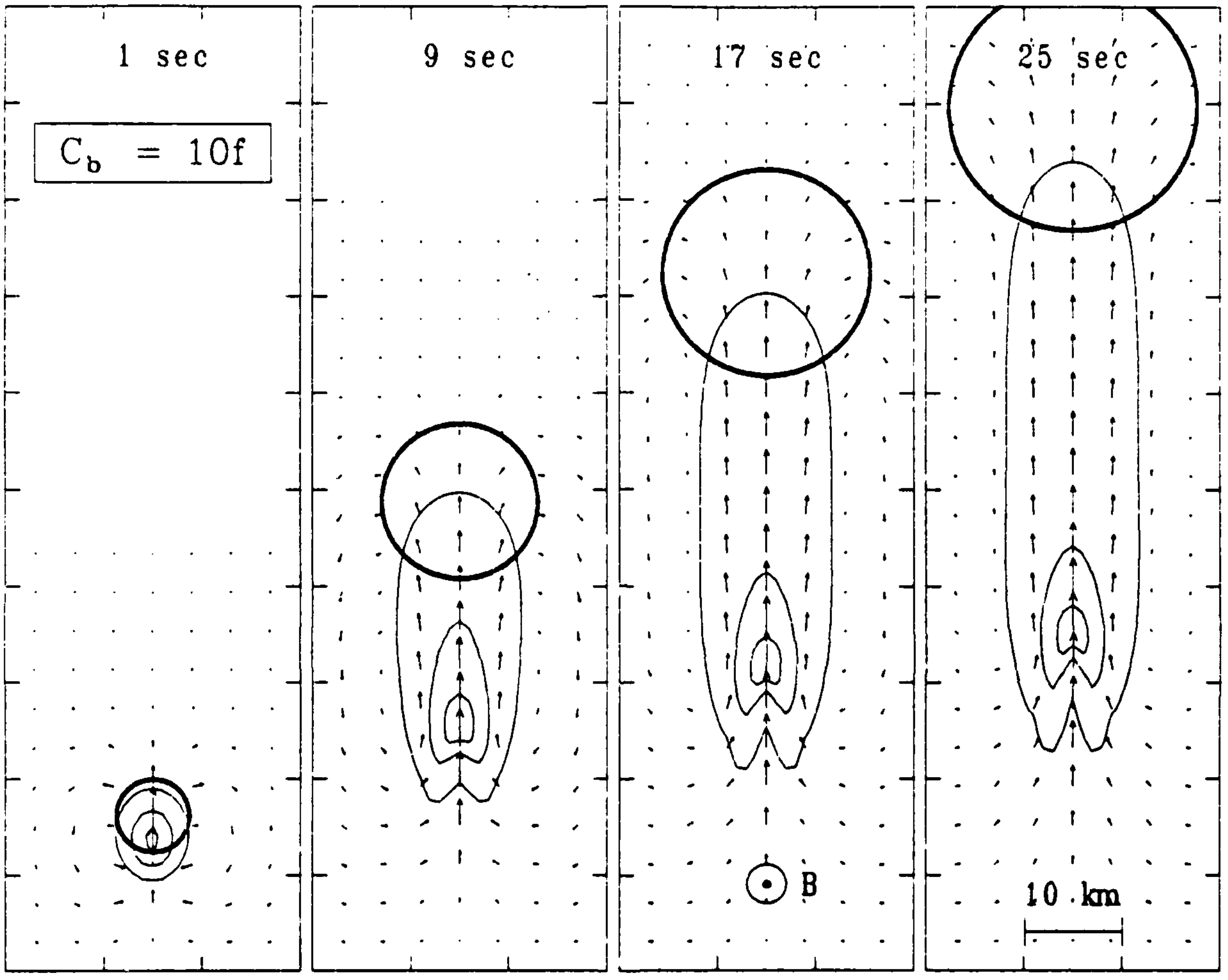

Fig. 2 — Same as Figure 1 for the case $C_b = 10$ f. (a) Contours of constant Σ_{pc} and velocity flow vectors. (b) Electrostatic potential contours.

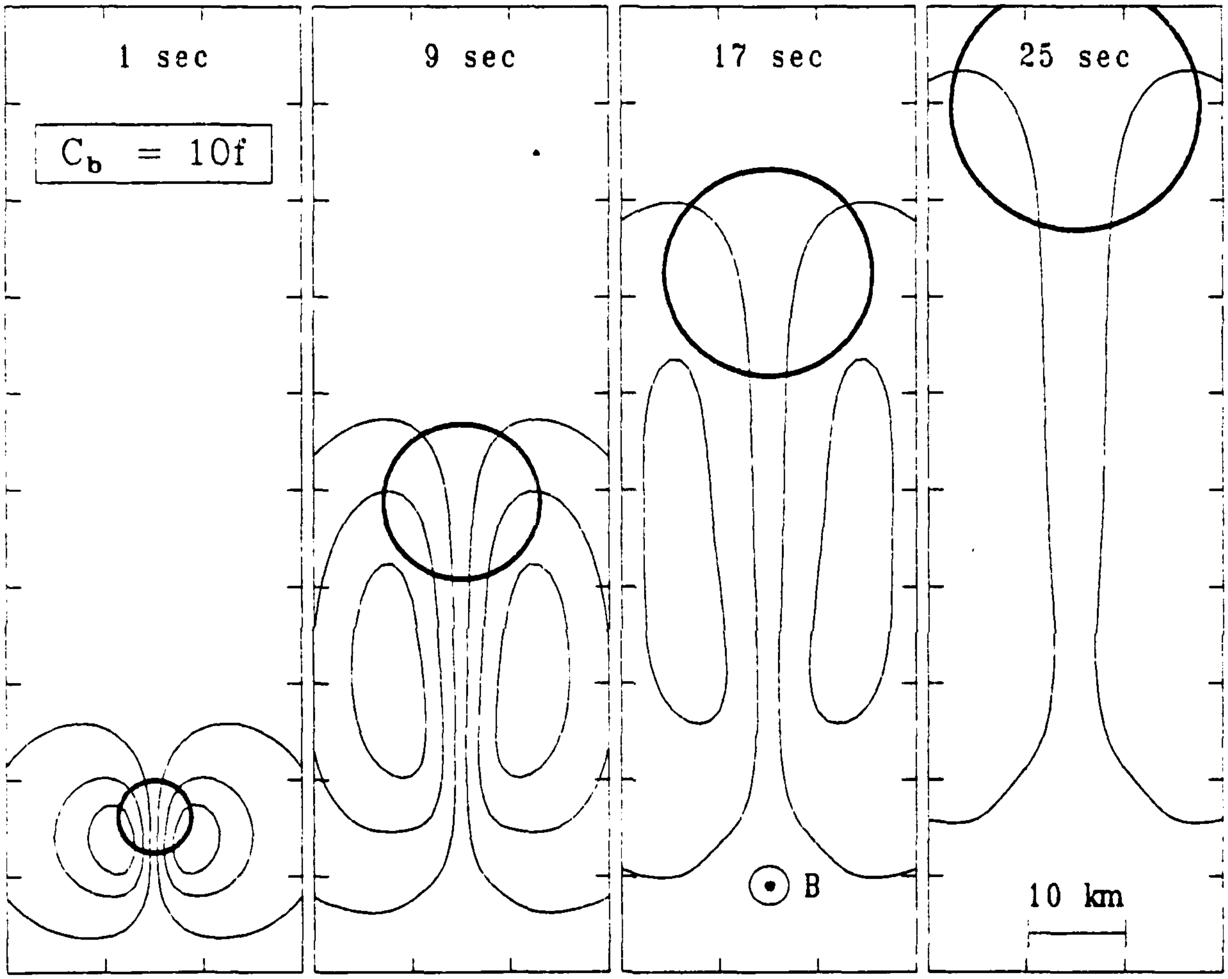

Fig. 2 (Cont'd) — Same as Figure 1 for the case C_b = 10 f. (a) Contours of constant Σ_{pc} and velocity flow vectors. (b) Electrostatic potential contours.

References

Brence, W.A., R.E. Carr, J.C. Gerlach, and H. Neuss, NASA/Max Planck Institute Barium Ion Cloud Project, J. Geophys. Res., 78, 5726, 1973.

Goertz, C.K., Io's interaction with the plasma torus, J. Geophys. Res., 85, 2949-2956, 1980.

Hain, K., A non-recursive incomplete Cholesky decomposition method for the solution of linear equations with a sparse matrix, NRL Memorandum Report 4264, Naval Research Laboratory, Washington, D.C., 1980.

Heppner, J.P., M.L. Miller, M.B. Pongratz, G.M. Smith, L.L. Smith, S.B. Mende, and N.R. Nath, The Cameo barium releases: $E_{\parallel}$ fields over the polar cap, J. Geophys. Res., 86, 3519, 1981.

Koons, H.C. and M.B. Pongratz, Electric fields and plasma waves resulting from a barium injection experiment, J. Geophys. Res., 86, 1437, 1981.

McDonald, B.E., S.L. Ossakow, S.T. Zalesak, and N.J. Zabusky, Scale sizes and lifetimes of F region plasma cloud striations as determined by the condition of marginal stability, J. Geophys. Res., 86, 5775, 1981.

Mende, S.B., Morphology of the magnetospheric barium release, J. Geophys. Res., 78, 5751, 1973.

Mitchell, H.G., J.A. Fedder, M.J. Keskinen, and S.T. Zalesak, "A simulation of high latitude F-layer instabilities in the presence of magnetosphere-ionosphere coupling," Geophys. Res. Lett., 12, 283, 1985.

Scholer, M., On the motion of artificial ion clouds in the magnetosphere, Planet. Space Sci., 18, 977, 1970.

Simons, D.J., M.B. Pongratz, and S. P. Gary, Prompt Striations in Ionospheric barium clouds due to a velocity space instability, J. Geophys. Res., 85, 671, 1980.

Sperling, J.L., Ion-Pederson drift and parallel electric field effects on plasma jetting, J. Geophys. Res., 88, 7095. 1983.

Wescott, E.M., H.C. Stenbaek-Nielsen, T.J. Hallinan, C.S. Deehr, F.J. Romick, J.V. Olson, J.G. Roederer, and R. Sydora, "A high-altitude barium radial injection experiiment," Geophys. Res. Lett., 1, 1037, 1980.

Zalesak, S.T., S.L. Ossakow, and P.K. Chaturvedi, Nonlinear equatorial spread F: the effect of neutral winds and background Pedersen conductivity, J. Geophys. Res., 87, 151, 1982.

Zalesak, S.T., P.K. Chaturvedi, S.L. Ossakow, and J.A. Fedder, Finite temperature effects on the evolution of ionospheric barium clouds in the presence of a conducting background ionosphere I. A high altitude incompressible background ionosphere, J. Geophys. Res., 90, 4299, 1985.

IONOSPHERIC MODELING DISTRIBUTION LIST
(UNCLASSIFIED ONLY)

PLEASE DISTRIBUTE ONE COPY TO EACH OF THE FOLLOWING PEOPLE (UNLESS OTHERWISE NOTED)

NAVAL RESEARCH LABORATORY
WASHINGTON, D.C. 20375
DR. S. OSSAKOW - Code 4700 (26 Copies)
Code 4701
Code 4780 (50 copies)
Code 4100
DR. H. GURSKY - CODE 4100
DR. J. GOODMAN - CODE 4180
DR. P. RODRIGUEZ - CODE 4706

A.F. GEOPHYSICS LABORATORY
L.G. HANSCOM FIELD
BEDFORD, MA 01731
DR. T. ELKINS
DR. W. SWIDER
MRS. R. SAGALYN
DR. J.M. FORBES
DR. T.J. KENESHEA
DR. W. BURKE
DR. H. CARLSON
DR. J. JASPERSE
Dr. F.J. RICH
DR. N. MAYNARD

BOSTON UNIVERSITY
DEPARTMENT OF ASTRONOMY
BOSTON, MA 02215
DR. J. AARONS

CORNELL UNIVERSITY
ITHACA, NY 14850
DR. W.E. SWARTZ
DR. R. SUDAN
DR. D. FARLEY
DR. M. KELLEY

HARVARD UNIVERSITY
HARVARD SQUARE
CAMBRIDGE, MA 02138
DR. M.B. McELROY
DR. R. LINDZEN

INSTITUTE FOR DEFENSE ANALYSIS
400 ARMY/NAVY DRIVE
ARLINGTON, VA 22202
DR. E. BAUER

MASSACHUSETTS INSTITUTE OF TECHNOLOGY
PLASMA FUSION CENTER
LIBRARY, NW16-262
CAMBRIDGE, MA 02139

NASA
GODDARD SPACE FLIGHT CENTER
GREENBELT, MD 20771
DR. R.F. BENSON
DR. K. MAEDA
Dr. S. CURTIS
Dr. M. DUBIN

COMMANDER
NAVAL AIR SYSTEMS COMMAND
DEPARTMENT OF THE NAVY
WASHINGTON, D.C. 20360
DR. T. CZUBA

COMMANDER
NAVAL OCEAN SYSTEMS CENTER
SAN DIEGO. CA 92152
MR. R. ROSE - CODE 5321

NOAA
DIRECTOR OF SPACE AND ENVIRONMENTAL LABORATORY
BOULDER, CO 80302
DR. A. GLENN JEAN
DR. G.W. ADAMS
DR. D.N. ANDERSON
DR. K. DAVIES
DR. R. F. DONNELLY

OFFICE OF NAVAL RESEARCH
800 NORTH QUINCY STREET
ARLINGTON, VA 22217
DR. G. JOINER

LABORATORY FOR PLASMA AND FUSION ENERGIES STUDIES
UNIVERSITY OF MARYLAND
COLLEGE PARK, MD 20742
JHAN VARYAN HELLMAN,
REFERENCE LIBRARIAN

PENNSYLVANIA STATE UNIVERSITY
UNIVERSITY PARK, PA 16802
DR. J.S. NISBET
DR. P.R. ROHRBAUGH
DR. L.A. CARPENTER
DR. M. LEE
DR. R. DIVANY
DR. P. BENNETT
DR. F. KLEVANS

PRINCETON UNIVERSITY
PLASMA PHYSICS LABORATORY
PRINCETON, NJ 08540
DR. F. PERKINS

SCIENCE APPLICATIONS, INC.
1150 PROSPECT PLAZA
LA JOLLA, CA 92037
DR. D.A. HAMLIN
DR. L. LINSON
DR. E. FRIEMAN

STANFORD UNIVERSITY
STANFORD, CA 94305
DR. P.M. BANKS

U.S. ARMY ABERDEEN RESEARCH
AND DEVELOPMENT CENTER
BALLISTIC RESEARCH LABORATORY
ABERDEEN, MD
DR. J. HEIMERL

GEOPHYSICAL INSTITUTE
UNIVERSITY OF ALASKA
FAIRBANKS, AK 99701
DR. L.C. LEE

UNIVERSITY OF CALIFORNIA
LOS ALAMOS SCIENTIFIC LABORATORY
J-10, MS-664
LOS ALAMOS, NM 87545
DR. M. PONGRATZ
DR. D. SIMONS
DR. G. BARASCH
DR. L. DUNCAN
DR. P. BERNHARDT
DR. S.P. GARY

UNIVERSITY OF ILLINOIS
DEPT. OF ELECTRICAL ENGINEERING
1406 W. GREEN STREET
URBANA, IL 61801
DR. ERHAN KUDEKI

UNIVERSITY OF CALIFORNIA,
LOS ANGELES
405 HILLGARD AVENUE
LOS ANGELES, CA 90024
DR. F.V. CORONITI
DR. C. KENNEL
DR. A.Y. WONG

UNIVERSITY OF MARYLAND
COLLEGE PARK, MD 20740
DR. K. PAPADOPOULOS
DR. E. OTT

JOHNS HOPKINS UNIVERSITY
APPLIED PHYSICS LABORATORY
JOHNS HOPKINS ROAD
LAUREL, MD 20810
DR. R. GREENWALD
DR. C. MENG

UNIVERSITY OF PITTSBURGH
PITTSBURGH, PA 15213
DR. N. ZABUSKY
DR. M. BIONDI
DR. E. OVERMAN

UNIVERSITY OF TEXAS
AT DALLAS
CENTER FOR SPACE SCIENCES
P.O. BOX 688
RICHARDSON, TEXAS 75080
DR. R. HEELIS
DR. W. HANSON
DR. J.P. McCLURE

UTAH STATE UNIVERSITY
4TH AND 8TH STREETS
LOGAN, UTAH 84322
DR. R. HARRIS
DR. K. BAKER
DR. R. SCHUNK
DR. J. ST.-MAURICE

PHYSICAL RESEARCH LABORATORY
PLASMA PHYSICS PROGRAMME
AHMEDABAD 380 009
INDIA
P.J. PATHAK, LIBRARIAN

Director of Research
U.S. Naval Academy
Annapolis, MD 21402 (2 copies)

END

FILMED

10-85

DTIC